Pergamon

Int. J. Solids Structures Vol. 35, No. 7–8, pp. 573–592, 1998

0020–7683/98 $19.00 + .00

PII: S0020–1683(97)00068–1

COMPLEX-VALUED WAVENUMBER, REFLECTION AND TRANSMISSION IN AN ELASTIC SOLID CONTAINING A CRACKED SLAB REGION

Y. C. ANGEL and Y. K. KOBA
Department of Mechanical Engineering and Materials Science, Rice University—MS321, PO Box 1892, Houston, TX 77005-1892, U.S.A.

(*Received* 3 *September* 1996; *in revised form* 3 *March* 1997)

Abstract—Propagation of ultrasonic or seismic waves in an elastic solid where slit cracks are randomly distributed is investigated. The distribution has a uniform probability density in a slab region, the cracks are parallel to the boundaries of the slab, and the solid is uncracked on either side of the slab. When an antiplane wave is normally incident on the cracks, it is shown that the average (coherent) motion is governed by two coupled integral equations. These equations are solved assuming that the average exciting stress near a fixed crack is equal to the average total stress. Inside the slab, where multiple scattering occurs, there is a forward motion and a backward motion. The velocity and attenuation of the two motions are shown to be given by simple formulae that depend on frequency and crack density. Simple formulae, which depend on frequency, crack density, and slab thickness, are also obtained for the wave amplitudes outside the slab. Plots of the velocity, attenuation, reflected amplitude, and transmitted amplitude vs the frequency are presented for several values of crack density and slab thickness. Low and high frequency limits of these quantities are examined analytically and numerically. © 1997 Elsevier Science Ltd

1. INTRODUCTION

It has long been known from experimental observations that wave propagation through media containing distributed inhomogeneities (particles, defects, inclusions) is governed by a frequency-dependent complex-valued wavenumber, where the real and imaginary parts are measures respectively of wave velocity and attenuation. The complex-valued wavenumber describes approximately the overall (coherent) wave motion generated by multiple scattering effects; it acts as a device that smooths out local fluctuations.

If one assumes that real sensors naturally filter and smooth incoming signals, then one concludes that coherent wave motions (velocity and attenuation) are readily measurable in the laboratory. In recent years, velocity and attenuation measurements have been reported for electromagnetic waves by Kuga *et al.* (1996), for seismic waves in fractured rocks by Peacock *et al.* (1994a, b), and for waves in elastic solids by Kinra *et al.* (1980), Kinra and Anand (1982), and Sayers and Smith (1983).

What is not readily measurable is the incoherent motion, which represents fine-scale scattering effects and is defined as the difference between the actual and coherent motions. It is worth mentioning that conservation of energy does not hold for either the incoherent or coherent motion, but *does* hold for the sum of the two motions.

Analytical evidence that multiple-scattering effects generate complex-valued wavenumbers was provided by Foldy (1945), Lax (1951, 1952), Waterman and Truell (1961), and Twersky (1962). Their method, which has proved very useful, consists of evaluating the configuration-averaged motion through randomly distributed scatterers. One difficulty with this method, as observed by Groenenboom and Snieder (1995), is that it identifies the analytical average motion (over an ensemble of configurations) with the coherent motion (corresponding to only one configuration or measurement). Such an identification raises legitimate questions. A second difficulty is that the analytical evidence provided by Foldy, Lax, Waterman, Truell, and Twersky is applicable mostly to *point* scatterers, but not directly to finite-size scatterers. In this paper, we address the second difficulty.

Most often, for finite-size scatterers, physical arguments are invoked to justify the use of a complex-valued wavenumber. This is the case in McCarthy and Carroll (1984), Varadan *et al.* (1989), Kerr (1992), and Bose (1996) for cylindrical or spherical inclusions; and in Kikuchi (1981a, b), Angel and Achenbach (1991), Zhang and Achenbach (1991), Zhang and Gross (1993a, b), Angel and Koba (1993), and Eriksson *et al.* (1995) for cracks. These authors, except Kikuchi (1981a, b), determine the complex-valued wavenumber indirectly by using various analytical and numerical methods, such as an energy method together with a Kramers–Kronig relation. Kikuchi (1981a, b) derives a result of particular interest: a simple explicit formula for the complex-valued wavenumber.

Backward motions, reflection, and transmission have been examined only in Waterman and Truell (1961), Twersky (1962), and Bose (1996). In other papers, attention is confined to the forward motion.

In this paper, which is based on the doctoral dissertation of Koba (1996), we obtain simple explicit expressions, which were not available before, for the backward motion, reflection, and transmission in an elastic solid containing a randomly-cracked slab region. These expressions will be of interest in ultrasonic nondestructive evaluation and seismic exploration.

We obtain the configuration-averaged motion, inside and outside the slab, by using a new approach that consists of averaging the exact equations of motion and crack boundary conditions. The formulation is presented in Sections 2 and 3. The cracks are identical and parallel to the boundaries of the slab, and an antiplane wave is normally incident on the cracks. In Section 4, we derive governing equations for the N-crack problem, when the N cracks are contained in a rectangle of the slab region. Then, we average these equations. This allows us to express in (18) the average total motion in terms of the average motion scattered by a fixed crack, which itself depends on the average exciting motion near the same fixed crack.

Next, in Section 5, we take the limit of (18) as the rectangle approaches the slab region, keeping the density of cracks per unit area constant. This limit process yields eqn (36), which expresses the average total motion in terms of a density function b. The density function b satisfies the singular integral eqn (37). With eqns (36) and (37), provided that the average exciting displacement near a fixed crack is known, one can evaluate the configuration-averaged motion inside and outside the slab.

In Section 6, we examine eqns (36) and (37) in the special case where the average exciting displacement near a fixed crack is equal to the average total displacement. Under these circumstances, we find that there is a forward motion and a backward motion that propagate in the cracked region with complex-valued wavenumbers $\pm K$. The wavenumber K is determined explicitly in terms of frequency and crack density by eqn (48). Outside the slab, eqns (36) and (37) yield expressions for the amplitudes R and T of the reflected and transmitted motions.

We observe that the wavenumber K does not depend on the thickness h of the slab for finite values of h. In contrast, the amplitudes C and D of the forward and backward waves inside the cracked region, as well as the transmission coefficient T and the reflection coefficient R, depend on the thickness h. The formulae for C, D, T, and R are labeled (50), (51), (57), and (58), respectively. The velocity and attenuation, which are obtained respectively from the real and imaginary parts of the complex-valued wavenumber, are given in eqn (72).

In Section 7, we find the limits of the velocity and attenuation for small crack density. Our results are identical to those of Angel and Koba (1993), who used an energy method and a Kramers–Kronig relation. In the limit of small crack density, the backward wave in the cracked region is negligible in comparison with the forward wave.

We also determine analytically the velocity and attenuation in the limit of zero frequency. This calculation shows that our results are valid for small (and possibly moderate) values of the crack density. Finally, we discuss the numerical method of solution in Section 8, and we present plots of the velocity, attenuation, reflection coefficient, and transmission coefficient vs the frequency for several values of crack density and slab thickness.

2. FORMULATION

We consider a linearly elastic, homogeneous, and isotropic solid that contains a random distribution of parallel cracks, as shown in Fig. 1. The cracks have width $2a$, lie in planes orthogonal to the (y_1, y_2) plane, extend to infinity in the $\pm y_3$ directions, and their centers are contained in the open slab V_∞^h of width $2h$ defined by

$$V_\infty^h = \{(y_1, y_2) \in \mathbb{R}^2 : |y_1| < \infty, |y_2| < h\}. \tag{1}$$

Let $\mathbf{e}_\alpha$ ($\alpha = 1, 2$) be orthonormal base vectors attached to the axes y_α, respectively, and let ζ be the position vector of a crack center. Then, since ζ is a point of V_∞^h, one has

$$\zeta = \zeta_1 \mathbf{e}_1 + \zeta_2 \mathbf{e}_2, \quad (|\zeta_2| < h). \tag{2}$$

We attach at ζ a system of orthogonal axes (x_1, x_2) such that the x_1 axis lies along the crack face. The x_1 and the y_1 axes are parallel to each other. The transformation of coordinates from the (y_1, y_2) coordinate system to the (x_1, x_2) system is given by

$$x_1 = y_1 - \zeta_1, \tag{3}$$

$$x_2 = y_2 - \zeta_2. \tag{4}$$

Let ρ and μ denote, respectively, the mass density and the shear modulus of the solid. Then, the speed c_T and the slowness s_T of transverse waves are given by

$$c_T^2 = \mu/\rho, \quad s_T = 1/c_T. \tag{5}$$

An antiplane wave is incident on the cracks and propagates along the y_2 direction. The displacement u^{inc}, which is in the y_3 direction, is given by

$$u^{inc}(y_2) = u_0 \exp(iky_2), \quad k = \omega s_T, \tag{6}$$

where the time-harmonic factor, $\exp(-i\omega t)$, is omitted. In (6), u_0 is the amplitude and ω is the frequency.

The incident wave (6) is subjected to multiple reflections between the cracks. A first encounter with a crack produces a first-order scattered wave, which propagates in all directions away from the crack and encounters the other cracks, thus producing second-order scattered waves. Eventually, scattered waves of all orders, up to infinity, are generated. In a steady-state regime, the time-harmonic factor, $\exp(-i\omega t)$, is common to all incident and scattered fields; it will be omitted throughout this work.

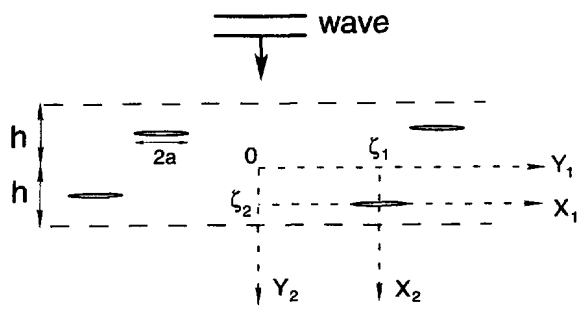

Fig. 1. Uniform distribution of parallel cracks in an unbounded elastic solid.

3. UNIFORM DISTRIBUTION OF CRACKS

The cracks in the slab V_∞^h are randomly distributed. Thus, the crack-center positions are known in a probabilistic sense only, and the probability that a crack be located at a given point in V_∞^h is independent of the particular point chosen. It follows that the number n of cracks per unit area in V_∞^h is constant on average, and the distribution is uniform in V_∞^h. We construct a sequence of bounded open rectangles $\{V_N^h\}$, where N is a sufficiently large integer, such that

$$V_N^h = \left\{(y_1, y_2) \in \mathbb{R}^2 : |y_1| < \frac{N}{4hn}, |y_2| < h\right\}. \tag{7}$$

Since the area of V_N^h is N/n, the rectangle V_N^h contains N cracks. Further, the rectangle V_N^h is contained in V_∞^h and approaches V_∞^h as N approaches infinity. Let Ω^{2N} be the N-fold Cartesian product of V_N^h. When the N crack centers $\zeta^1, \zeta^2, \ldots, \zeta^N$ are in V_N^h, then the $2N$-point $(\zeta_1^1, \zeta_2^1, \ldots, \zeta_1^N, \zeta_2^N)$ is in Ω^{2N}.

We define a probability density function $p: \Omega^{2N} \to \mathbb{R}$ for the configurations of the N crack centers $\zeta^1, \zeta^2, \ldots, \zeta^N$. Since the crack centers are contained in V_N^h, one has

$$\int_{\Omega^{2N}} p(\zeta^1, \ldots, \zeta^N)\, \mathrm{d}\zeta^1 \ldots \mathrm{d}\zeta^N = 1. \tag{8}$$

In addition, we assume that the N parallel cracks have no points of contact and that they are exchangeable. Thus, the function p takes the same value at $(\zeta^1, \ldots, \zeta^N)$ and at all other points in Ω^{2N} that differ from $(\zeta^1, \ldots, \zeta^N)$ by an arbitrary reordering of the N centers. Finally, since the distribution is uniform in V_N^h, the probability that a crack center be located at any point in the rectangle V_N^h is equal to one over the area of V_N^h. Thus, one has

$$\int_{\Omega^{2N-2}} p(\zeta^1, \ldots, \zeta^{i-1}, \mathbf{x}, \zeta^{i+1}, \ldots, \zeta^N)\, \mathrm{d}\zeta^1 \ldots \mathrm{d}\zeta^{i-1}\, \mathrm{d}\zeta^{i+1} \ldots \mathrm{d}\zeta^N = \frac{n}{N}. \tag{9}$$

In the left-hand side of (9), the value of $\mathbf{x}$ can be chosen arbitrarily in V_N^h, and this leaves the value of the integral unchanged. Further, the position i occupied by $\mathbf{x}$ can be chosen arbitrarily since the cracks are exchangeable and the integration order is immaterial.

4. PROBABILISTIC N-CRACK PROBLEM

We consider N cracks centered in the rectangle V_N^h of (7) and subjected to the incident antiplane wave (6). Assuming that the cracks are distributed according to the uniform probability density function of Section 3, we obtain equations for the average wave motion in the solid.

The total displacement u^{T} in the solid is equal to the sum of the incident displacement u^{inc} and of the scattered displacements $\bar{u}^{\mathrm{sc}}$ corresponding to each of the N cracks. Thus, one has

$$u^{\mathrm{T}}(y_1, y_2 \mid \Lambda^N) = u^{\mathrm{inc}}(y_2) + \sum_{i=1}^{N} \bar{u}^{\mathrm{sc}}(y_1, y_2; \zeta^i \mid \Lambda^N), \tag{10}$$

where $\Lambda^N = (\zeta^1, \ldots, \zeta^N)$ denotes the configuration of cracks in the rectangle V_N^h. In (10), the scattered displacement of the ith crack is labeled with the position ζ^i after the semi-colon. The exciting displacement $\bar{u}^{\mathrm{E}}$ on the ith crack is equal to the total displacement minus the ith scattered displacement. Thus, one has

$$\bar{u}^{\mathrm{E}}(y_1, y_2; \zeta^i \mid \Lambda^N) = u^{\mathrm{T}}(y_1, y_2 \mid \Lambda^N) - \bar{u}^{\mathrm{sc}}(y_1, y_2; \zeta^i \mid \Lambda^N). \tag{11}$$

On the ith crack, we attach a system of coordinates (x_1^i, x_2^i), as in Section 2. Then, the transformation of coordinates from the (y_1, y_2) system to the (x_1^i, x_2^i) system is given by (3) and (4), where a superscript i is attached to the x and ζ variables. Using the local coordinates (x_1^i, x_2^i), we can define functions u^{sc} and u^{E} in terms of $\bar{u}^{\mathrm{sc}}$ and $\bar{u}^{\mathrm{E}}$ such that

$$u^{\mathrm{sc}}(x_1^i, x_2^i; \zeta^i \mid \Lambda^N) = \bar{u}^{\mathrm{sc}}(y_1, y_2; \zeta^i \mid \Lambda^N), \tag{12}$$

$$u^{\mathrm{E}}(x_1^i, x_2^i; \zeta^i \mid \Lambda^N) = \bar{u}^{\mathrm{E}}(y_1, y_2; \zeta^i \mid \Lambda^N). \tag{13}$$

The scattered displacement u^{sc} of the ith crack is discontinuous on the faces of the crack and is antisymmetric with respect to the x_1^i axis, which implies that u^{sc} vanishes on the x_1^i axis at all points that are not on the crack faces. This situation is identical to that of the one-crack problem discussed in Angel (1988). One can write N Helmholtz partial differential equations for the N scattered displacements u^{sc}. There are also N boundary conditions, which impose the vanishing of the total stress σ_{23} on the N crack faces. The N boundary conditions yield a coupled system of integral equations of order N for the N unknown crack-face displacements $u^{\mathrm{sc}}(\alpha, 0^+; \zeta^i \mid \Lambda^N)$. It is difficult to solve this system numerically with good accuracy, even for a small number of cracks. For a large number of randomly distributed cracks, one can use a probabilistic approach.

The average $\langle \bar{u}^{\mathrm{sc}} \rangle_N$ of the ith-crack scattered displacement $\bar{u}^{\mathrm{sc}}$ is obtained by using the probability density $p: \Omega^{2N} \to \mathbb{R}$ of Section 3 in the form

$$\langle \bar{u}^{\mathrm{sc}} \rangle_N(y_1, y_2) = \int_{\Omega^{2N}} \bar{u}^{\mathrm{sc}}(y_1, y_2; \zeta^i \mid \Lambda^N) p(\Lambda^N)\, \mathrm{d}\zeta^1 \ldots \mathrm{d}\zeta^N. \tag{14}$$

Observe that the integral in (14) is independent of i, because the N center positions in Λ^N can be reordered arbitrarily and the integration order is immaterial. To gain further insight into the displacement $\langle \bar{u}^{\mathrm{sc}} \rangle_N$ of (14), we use the condition that the probability density p is uniform. Thus, separating in (14) the ζ^i integration from the other integrations, one finds that

$$\langle \bar{u}^{\mathrm{sc}} \rangle_N(y_1, y_2) = \frac{n}{N} \int_{V_N^h} \langle \bar{u}^{\mathrm{sc}} \rangle_{N-1}(y_1, y_2; \zeta)\, \mathrm{d}\zeta. \tag{15}$$

In (15), $\langle \bar{u}^{\mathrm{sc}} \rangle_{N-1}$ is the average displacement scattered by a fixed crack and is given by

$$\langle \bar{u}^{\mathrm{sc}} \rangle_{N-1}(y_1, y_2; \zeta) = \frac{N}{n} \int_{\Omega^{2N-2}} \bar{u}^{\mathrm{sc}}(y_1, y_2; \zeta \mid \Lambda_0^N) p(\Lambda_0^N)\, \mathrm{d}\zeta^1 \ldots \mathrm{d}\zeta^{i-1}\, \mathrm{d}\zeta^{i+1} \ldots \mathrm{d}\zeta^N, \tag{16}$$

where

$$\Lambda_0^N = (\zeta^1, \ldots, \zeta^{i-1}, \zeta, \zeta^{i+1}, \ldots, \zeta^N). \tag{17}$$

In (16), the crack is fixed at ζ, and the integral is independent of the rank i occupied in Λ_0^N by the vector ζ because the cracks are exchangeable. Thus, the average $\langle \bar{u}^{\mathrm{sc}} \rangle_{N-1}$ is independent of the crack that is held fixed. The factor N/n in front of the integral in (16) allows us, in view of (9), to call $\langle \bar{u}^{\mathrm{sc}} \rangle_{N-1}$ an average function.

We define the average $\langle u^{\mathrm{T}} \rangle_N$ of the total displacement u^{T} by using the same integration procedure as in (14). Integrating (10) times $p(\Lambda^N)$ over Ω^{2N}, and using (15), the independence of the average displacement $\langle \bar{u}^{\mathrm{sc}} \rangle_N$ on the index of the scattering crack, and also the normalization condition (8), one infers that

$$\langle u^{\mathrm{T}}\rangle_N(y_1,y_2) = u^{\mathrm{inc}}(y_2) + n\int_{V_N^h} \langle \bar{u}^{\mathrm{sc}}\rangle_{N-1}(y_1,y_2;\zeta)\,\mathrm{d}\zeta. \tag{18}$$

Equation (18) shows that $\langle u^{\mathrm{T}}\rangle_N$ depends on the average displacement $\langle \bar{u}^{\mathrm{sc}}\rangle_{N-1}$ scattered by a fixed crack.

One can write $\langle \bar{u}^{\mathrm{sc}}\rangle_{N-1}$ in terms of averages of $\bar{u}^{\mathrm{sc}}$ with two, three, or more cracks held fixed, if one knows the successive conditional probability density functions when the number of fixed cracks runs from 2 to $N-1$. In this paper, we consider only the statistical information that corresponds to one crack held fixed, as given in (9).

5. PROBABILISTIC SLAB PROBLEM

We now derive equations for the average total displacement in an elastic solid that contains the cracked slab V_∞^h of (1) and that is excited by the antiplane wave u^{inc} of (6). Since the rectangle V_N^h of Section 3 approaches V_∞^h as N increases without bound, we take the limit of (18) as N approaches infinity, keeping the density n of cracks per unit area constant.

We assume that $\langle u^{\mathrm{T}}\rangle_N$ and $\langle \bar{u}^{\mathrm{sc}}\rangle_{N-1}$ have limits as N tends to infinity, for fixed values of the coordinates (y_1,y_2) and of the crack-center position ζ. In the limit, since the slab is infinite in the y_1 direction and the crack distribution is uniform, the average total displacement takes the same value at (y_1,y_2) and at (y_1+q,y_2), where q is an arbitrary real number. Also, in the limit, the average scattered displacement at (y_1,y_2) corresponding to a crack fixed at ζ is identical to the average scattered displacement at (y_1+q,y_2) corresponding to a crack fixed at $\zeta+q\mathbf{e}_1$, where q is an arbitrary real number and $\mathbf{e}_1$ is the unit base vector attached to the y_1 axis. Thus, we define the limits $\langle u^{\mathrm{T}}\rangle_\infty$ and $\langle \bar{u}^{\mathrm{sc}}\rangle_\infty$ such that

$$\langle u^{\mathrm{T}}\rangle_\infty(y_2) = \lim_{N\to\infty} \langle u^{\mathrm{T}}\rangle_N(y_1,y_2), \tag{19}$$

$$\langle \bar{u}^{\mathrm{sc}}\rangle_\infty(0,y_2;\zeta-y_1\mathbf{e}_1) = \langle \bar{u}^{\mathrm{sc}}\rangle_\infty(y_1,y_2;\zeta) = \lim_{N\to\infty} \langle \bar{u}^{\mathrm{sc}}\rangle_{N-1}(y_1,y_2;\zeta). \tag{20}$$

It follows now from (19) and (18) that the integral in (18) has a limit as N tends to infinity, and the limit is independent of the coordinate y_1. Next, we assume that the limit in (20) is reached uniformly with respect to the position ζ in each finite rectangle contained in V_∞^h. This allows us to interchange the limit and integration operations in the integral of (18). Thus, taking the limit of (18) as N tends to infinity, interchanging the limit and integration operations, using (19) and (20), and changing the ζ_1 integration variable that runs along the entire real axis, one infers that

$$\langle u^{\mathrm{T}}\rangle_\infty(y_2) = u^{\mathrm{inc}}(y_2) + n\int_{V_\infty^h} \langle \bar{u}^{\mathrm{sc}}\rangle_\infty(0,y_2;\zeta)\,\mathrm{d}\zeta. \tag{21}$$

Next, we define the limit $\langle u^{\mathrm{sc}}\rangle_\infty$ in terms of $\langle \bar{u}^{\mathrm{sc}}\rangle_\infty$ by using the change of coordinates (3) and (4). Since the slab is infinite in the y_1 direction and the crack distribution is uniform, the average scattered displacement $\langle u^{\mathrm{sc}}\rangle_\infty$ evaluated at a fixed point (x_1,x_2) in local coordinates takes the same value when the crack is centered at (ζ_1,ζ_2) and when it is centered at (ζ_1+q,ζ_2), where q is an arbitrary real number. Thus, we write

$$\langle u^{\mathrm{sc}}\rangle_\infty(x_1,x_2;\zeta_2) = \langle u^{\mathrm{sc}}\rangle_\infty(x_1,x_2;\zeta) = \langle \bar{u}^{\mathrm{sc}}\rangle_\infty(y_1,y_2;\zeta). \tag{22}$$

We recall that, for N cracks occupying deterministic positions in V_N^h, one can write N Helmholtz partial differential equations for the N scattered displacements u^{sc}. There are also N boundary conditions, which impose the vanishing of the total stress σ_{23} on the N crack faces and the vanishing of the scattered displacement of order i ($i=1,\ldots,N$) in the

plane $x_2^i = 0$ for $|x_1^i| \geqslant a$. If for each i we multiply these equations by $(N/n)p$ and integrate over the region Ω^{2N-2}, keeping the ith crack position fixed, and assuming that the integration and the differentiations can be interchanged, we obtain N identical differential equations and N identical boundary conditions. Thus, eliminating the unnecessary superscript i, we can denote by ζ the position of a fixed crack and by (x_1, x_2) the axes attached to the fixed crack. In the limit as $N \to \infty$, assuming that the limit operation and the differentiations can be interchanged and using (22), we find that the Helmholtz equation for the average scattered displacement is

$$\langle u^{sc}\rangle_{\infty,\alpha\alpha}(x_1, x_2; \zeta_2) + k^2 \langle u^{sc}\rangle_{\infty}(x_1, x_2; \zeta_2) = 0, \quad x_2 > 0. \tag{23}$$

In eqn (23), the derivatives are taken with respect to the coordinates x_1 and x_2 and a summation is implied over the repeated index α. The boundary conditions for the average scattered displacement are given in terms of the average exciting displacement $\langle u^E\rangle_\infty$ by

$$\frac{\partial}{\partial x_2}\langle u^{sc}\rangle_{\infty}(x_1, x_2; \zeta_2)|_{x_2=0^+} = -\frac{\partial}{\partial x_2}\langle u^{E}\rangle_{\infty}(x_1, x_2; \zeta_2)|_{x_2=0}, \quad |x_1| < a, \tag{24}$$

$$\langle u^{sc}\rangle_{\infty}(x_1, 0; \zeta_2) = 0, \quad |x_1| \geqslant a. \tag{25}$$

In (24), the average exciting displacement is obtained by using (11), the averaging procedure (16), and equations analogous to (20) and (22).

The displacement $\langle u^{sc}\rangle_\infty$ is antisymmetric with respect to the x_1 axis. Thus, we can define, as in Angel (1988), a function b in the interval $(-a, a) \times (-h, h)$ such that

$$\langle u^{sc}\rangle_{\infty}(x_1, 0^+; \zeta_2) = \begin{cases} \displaystyle\int_{-a}^{x_1} b(v; \zeta_2)\, dv, & |x_1| < a, \\ 0, & |x_1| \geqslant a, \end{cases} \tag{26}$$

together with

$$\int_{-a}^{a} b(v; \zeta_2)\, dv = 0. \tag{27}$$

In eqns (26) and (27), the parameter ζ_2 is such that $|\zeta_2| < h$, as in (2). Then, we can use the differential eqn (23) and eqns (26) and (27) to represent the displacement $\langle u^{sc}\rangle_\infty$ in terms of the function b. The result is

$$\langle u^{sc}\rangle_{\infty}(x_1, x_2; \zeta_2) = \frac{\operatorname{sgn}(x_2)}{\pi}\int_0^{\infty}\left\{\int_{-a}^{a} b(v; \zeta_2) L(x_1 - v, x_2, \xi)\, dv\right\} d\xi. \tag{28}$$

In (28), the integrand L is given by

$$L(x_1, x_2, \xi) = \frac{\sin(\xi x_1)}{\xi}\exp(-\beta|x_2|), \tag{29}$$

where β is defined by

$$\beta^2 = \xi^2 - k^2, \quad \operatorname{Im}(\beta) \leqslant 0, \quad \operatorname{Re}(\beta) \geqslant 0. \tag{30}$$

The displacement $\langle \bar{u}^{sc}\rangle_\infty(0, y_2; \zeta)$ inside the integral of (21) can be written in terms of the function b by using (28), (22), and the change of coordinates (3) and (4) with y_1 set equal to zero. Thus, one has

$$\langle \bar{u}^{sc} \rangle_\infty (0, y_2; \zeta) = \frac{1}{\pi} \operatorname{sgn}(y_2 - \zeta_2) \int_{-a}^{a} b(v; \zeta_2) P(v, y_2, \zeta) \, dv, \tag{31}$$

where the integral P is defined by

$$P(v, y_2, \zeta) = \int_0^\infty L(-\zeta_1 - v, y_2 - \zeta_2, \xi) \, d\xi. \tag{32}$$

Substituting (31) into (21), one finds that the average total displacement $\langle u^T \rangle_\infty$ can be expressed in terms of the function b. The result is

$$\langle u^T \rangle_\infty (y_2) = u^{inc}(y_2) + \frac{n}{\pi} \int_{-h}^{h} \left\{ \int_{-a}^{a} b(v; \zeta_2) J(v, y_2, \zeta_2) \, dv \right\} d\zeta_2. \tag{33}$$

The integral J in (33) is defined by

$$J(v, y_2, \zeta_2) = \operatorname{sgn}(y_2 - \zeta_2) \lim_{X \to \infty} \int_{-X}^{X} P(v, y_2, \zeta) \, d\zeta_1. \tag{34}$$

It is shown in the Appendix that the integral J can be evaluated in closed form. The result is

$$J(v, y_2, \zeta_2) = -\pi v \operatorname{sgn}(y_2 - \zeta_2) \exp(ik|y_2 - \zeta_2|). \tag{35}$$

Substituting (35) into (33), one finds that $\langle u^T \rangle_\infty$ is given by

$$\langle u^T \rangle_\infty (y_2) = u^{inc}(y_2) - n \int_{-h}^{h} \left\{ \int_{-a}^{a} v b(v; \zeta_2) \, dv \right\} \operatorname{sgn}(y_2 - \zeta_2) \exp(ik|y_2 - \zeta_2|) \, d\zeta_2. \tag{36}$$

Using the boundary condition (24) and the representation (28), one finds, as in Angel (1988), that b satisfies a singular integral equation. This equation has the form

$$\int_{-a}^{a} b(v; \zeta_2) \left[\frac{1}{v - x_1} + S(v - x_1) \right] dv = -\pi \frac{\partial}{\partial x_2} \langle u^E \rangle_\infty (x_1, x_2; \zeta_2)|_{x_2 = 0}, \quad |x_1| < a. \tag{37}$$

In (37), the function S is given by

$$S(x) = \int_0^\infty \left(\frac{\beta}{\xi} - 1 \right) \sin(\xi x) \, d\xi. \tag{38}$$

Equation (37), together with (27), can be solved for $b(v; \zeta_2)$ when the exciting displacement $\langle u^E \rangle_\infty$ is known near the crack faces.

6. COMPLEX-VALUED WAVENUMBER

We now assume that, in a small neighborhood of a fixed crack, the average exciting displacement is equal to the average total displacement. Thus, using the correspondence (22) and the coordinate transformation (4), we write

$$\langle u^{\mathrm{E}}\rangle_\infty(x_1,x_2;\zeta_2)=\langle \bar{u}^{\mathrm{E}}\rangle_\infty(y_1,y_2;\boldsymbol{\zeta})=\langle u^{\mathrm{T}}\rangle_\infty(y_2)=\langle u^{\mathrm{T}}\rangle_\infty(\zeta_2+x_2). \tag{39}$$

Substituting (39) into (37), and using a prime superscript to denote the derivative, one finds that

$$\int_{-a}^{a} b(v;\zeta_2)\left[\frac{1}{v-x_1}+S(v-x_1)\right]\mathrm{d}v=-\pi\langle u^{\mathrm{T}}\rangle'_\infty(\zeta_2),\quad |x_1|<a. \tag{40}$$

It follows from (40) that the ratio of $b(v;\zeta_2)$ to $\langle u^{\mathrm{T}}\rangle'_\infty(\zeta_2)$ does not depend on ζ_2. Thus, we define a function b that depends only on v such that

$$b(v;\zeta_2)=b(v)\langle u^{\mathrm{T}}\rangle'_\infty(\zeta_2),\quad (|\zeta_2|<h). \tag{41}$$

The function $b(v)$ in (41) satisfies equations that follow directly from (40) and (27). These equations are

$$\int_{-a}^{a} b(v)\left[\frac{1}{v-x_1}+S(v-x_1)\right]\mathrm{d}v=-\pi,\quad |x_1|<a, \tag{42}$$

$$\int_{-a}^{a} b(v)\,\mathrm{d}v=0. \tag{43}$$

Next, we substitute (41) and (6) into (36) and we find that the average total displacement has the form

$$\langle u^{\mathrm{T}}\rangle_\infty(y_2)=u_0\exp(iky_2)-nBa^2\int_{-h}^{h}\langle u^{\mathrm{T}}\rangle'_\infty(\alpha)\,\mathrm{sgn}(y_2-\alpha)\exp(ik|y_2-\alpha|)\,\mathrm{d}\alpha, \tag{44}$$

where B is a complex-valued number that is defined by

$$Ba^2=\int_{-a}^{a} vb(v)\,\mathrm{d}v. \tag{45}$$

Differentiating (44) twice in the range $|y_2|<h$, and using the result that the derivative of the sign function is equal to twice the Dirac delta function, we find that

$$(1+2na^2B)\langle u^{\mathrm{T}}\rangle''_\infty(y_2)+k^2\langle u^{\mathrm{T}}\rangle_\infty(y_2)=0,\quad (|y_2|<h). \tag{46}$$

Equation (46) is a second-order ordinary differential equation with complex-valued coefficients. The general solution of this equation is

$$\langle u^{\mathrm{T}}\rangle_\infty(y_2)=C\exp(iKy_2)+D\exp(-iKy_2), \tag{47}$$

where C and D are complex-valued constants, and K is a complex-valued wavenumber. The wavenumber K is given by

$$K^2=k^2/(1+2na^2B). \tag{48}$$

Observe now that $\mathrm{Im}(K^2)$ and $-\mathrm{Im}(B)$ have the same sign. Since $\mathrm{Im}(B)$ is negative for all frequencies, as will be seen in the next section, it follows that K^2 lies in the upper complex plane. For definiteness, we define K to be the complex root of K^2 that lies in the first

quadrant. Therefore, K has positive real and imaginary parts. We write the complex-valued wavenumber K in the form

$$K = \frac{\omega}{c} + i\alpha, \quad (c > 0, \alpha > 0), \tag{49}$$

where ω is the frequency, c is a velocity, and α is an attenuation coefficient. Using (49), we infer that the first term in (47) represents a forward wave; its velocity is c in the positive y_2 direction, and its amplitude has a relative rate of decay equal to α as y_2 increases. The second term in (47) is a backward wave; its velocity is c in the negative y_2 direction, and its amplitude has a relative rate of decay equal to α as y_2 decreases.

To determine the constants C and D of (47), it suffices to substitute (47) into (44). A simple integration, together with (48), shows that the terms containing $\exp(iKy_2)$ and $\exp(-iKy_2)$ in the right-hand side of (44) cancel those in the left-hand side. There remain a term with the factor $\exp(iky_2)$ plus a term with the factor $\exp(-iky_2)$. Since this sum must be zero for all values of y_2 in the range $|y_2| < h$, the constants that multiply $\exp(iky_2)$ and $\exp(-iky_2)$ vanish identically. This yields a linear system of two equations for C and D. The solution of this system is

$$C = 2u_0K(K+k)\exp[-i(K-k)h]/\Delta, \tag{50}$$

$$D = -2u_0K(K-k)\exp[i(K+k)h]/\Delta, \tag{51}$$

$$\Delta = (K+k)^2\exp[-2i(K-k)h] - (K-k)^2\exp[2i(K+k)h]. \tag{52}$$

In the range $|y_2| > h$, eqn (44) has the form

$$\langle u^T\rangle_\infty(y_2) = u_0T\exp(iky_2), \quad y_2 > h, \tag{53}$$

$$\langle u^T\rangle_\infty(y_2) = u_0\exp(iky_2) + u_0R\exp(-iky_2), \quad y_2 < -h, \tag{54}$$

where the transmission coefficient T and the reflection coefficient R are given by

$$u_0T = u_0 - nBa^2\int_{-h}^{h}\langle u^T\rangle'_\infty(\alpha)\exp(-ik\alpha)\,d\alpha, \tag{55}$$

$$u_0R = nBa^2\int_{-h}^{h}\langle u^T\rangle'_\infty(\alpha)\exp(ik\alpha)\,d\alpha. \tag{56}$$

Substituting (47), (48), (50), and (51) into (55) and (56), and evaluating the integrals, one finds that

$$T = 4kK/\Delta, \tag{57}$$

$$R = (K^2-k^2)[\exp(-2iKh) - \exp(2iKh)]/\Delta, \tag{58}$$

where Δ is defined in (52). It can be seen from (44) that the displacement $\langle u^T\rangle_\infty(y_2)$ is continuous at $y_2 = \pm h$, and the derivative $\langle u^T\rangle'_\infty(y_2)$ has finite discontinuities at $y_2 = \pm h$. The quantity $\mu(1+2na^2B)\langle u^T\rangle'_\infty$, which can be interpreted as an equivalent average stress, is continuous at the slab boundaries if n is set equal to zero outside the slab.

We now write the basic equations of the problem in dimensionless form. For this purpose, we introduce the following notations

$$\tilde{\omega} = \omega s_T a, \quad \tilde{c} = c/c_T, \quad \tilde{\alpha} = \alpha a, \quad \tilde{K} = Ka, \tag{59}$$

$$\varepsilon = na^2, \quad \tilde{h} = h/a, \quad \tilde{y}_2 = y_2/a, \quad x = x_1/a, \tag{60}$$

$$\tilde{b}(v) = b(av), \quad \tilde{S}(x) = aS(ax), \quad \tilde{\beta}^2(u) = u^2 - 1, \quad \mathrm{Im}(\tilde{\beta}) \leqslant 0, \quad \mathrm{Re}(\tilde{\beta}) \geqslant 0. \tag{61}$$

Then, eqns (42) and (43) yield

$$\int_{-1}^{1} \tilde{b}(v) \left[\frac{1}{v-x} + \tilde{S}(v-x) \right] \mathrm{d}v = -\pi, \quad |x| < 1, \tag{62}$$

$$\int_{-1}^{1} \tilde{b}(v)\, \mathrm{d}v = 0. \tag{63}$$

In eqn (62), the function $\tilde{S}$ is obtained from (38) and (61) and is given by

$$\tilde{S}(x) = \tilde{\omega} \int_0^{\infty} \left[\frac{\tilde{\beta}(u)}{u} - 1 \right] \sin(\tilde{\omega} u x)\, \mathrm{d}u. \tag{64}$$

From (48), (49) and (59)–(61), we infer that the dimensionless complex-valued wavenumber $\tilde{K}$ has the form

$$\tilde{K} = \frac{\tilde{\omega}}{\tilde{c}} + i\tilde{\alpha}, \quad \tilde{K}^2 = \tilde{\omega}^2/(1+2\varepsilon B), \quad (\tilde{c} > 0, \tilde{\alpha} > 0), \tag{65}$$

where B is now given by

$$B = \int_{-1}^{1} v\tilde{b}(v)\, \mathrm{d}v. \tag{66}$$

Using (59) and (60), we find that the constants C and D of (50) and (51) can be written in the form

$$C/u_0 = 2\tilde{K}(\tilde{K}+\tilde{\omega}) \exp[-i(\tilde{K}-\tilde{\omega})\tilde{h}]/\tilde{\Delta}, \tag{67}$$

$$D/u_0 = -2\tilde{K}(\tilde{K}-\tilde{\omega}) \exp[i(\tilde{K}+\tilde{\omega})\tilde{h}]/\tilde{\Delta}, \tag{68}$$

$$\tilde{\Delta} = (\tilde{K}+\tilde{\omega})^2 \exp[-2i(\tilde{K}-\tilde{\omega})\tilde{h}] - (\tilde{K}-\tilde{\omega})^2 \exp[2i(\tilde{K}+\tilde{\omega})\tilde{h}]. \tag{69}$$

Finally, the transmission and reflection coefficients T and R of (57) and (58) take the form

$$T = 4\tilde{\omega}\tilde{K}/\tilde{\Delta}, \tag{70}$$

$$R = (\tilde{K}^2 - \tilde{\omega}^2)[\exp(-2i\tilde{K}\tilde{h}) - \exp(2i\tilde{K}\tilde{h})]/\tilde{\Delta}. \tag{71}$$

Calculating from (65) the complex root of $\tilde{K}^2$ that lies in the first quadrant, one finds that the velocity $\tilde{c}$ and the attenuation $\tilde{\alpha}$ are given in terms of ε and B by

$$\tilde{c} = \sqrt{2}|1+2\varepsilon B|/Q, \quad \tilde{\alpha} = -2\varepsilon\tilde{\omega}\,\mathrm{Im}(B)/[\sqrt{2}|1+2\varepsilon B|Q], \tag{72}$$

where the vertical bars denote the complex modulus and the quantity Q is defined by

$$Q = [\mathrm{Re}(1+2\varepsilon B)+|1+2\varepsilon B|]^{1/2}. \tag{73}$$

7. LIMITS

For a fixed number n of cracks per unit area, the dimensionless parameter ε of (60) depends on crack size. For example, if every square of side $4a$ contains on average a crack of width $2a$, then $\varepsilon = 0.0625$. If in each square of side $4a$, there are on average 2 cracks (1 crack) of width a, then $\varepsilon = 0.03125$ ($\varepsilon = 0.015625$). For a large concentration of microcracks, such as that of 4 cracks of width $a/2$ in each square of side $4a$, then ε takes the value $\varepsilon = 0.015625$. These numerical examples show that the parameter ε takes in general small values less than 0.1.

When ε approaches zero, we can approximate the complex-valued wavenumber $\tilde{K}$ of (65) with the expression

$$\tilde{K} = \tilde{\omega}(1-\varepsilon B) = \tilde{\omega}[1-\varepsilon\,\mathrm{Re}(B)] - i\varepsilon\tilde{\omega}\,\mathrm{Im}(B). \tag{74}$$

Comparing (74) with the first equation of (65), we find that, in the limit as ε approaches zero, the velocity $\tilde{c}$ and the attenuation $\tilde{\alpha}$ are given by

$$\tilde{c} = 1+\varepsilon\,\mathrm{Re}(B), \quad \tilde{\alpha} = -\varepsilon\tilde{\omega}\,\mathrm{Im}(B), \quad \text{as } \varepsilon \to 0. \tag{75}$$

Since the real and imaginary parts of B are negative for all frequencies, as will be seen in the next section, we infer from (75) that $\tilde{c} < 1$ and $\tilde{\alpha} > 0$ as ε approaches zero. Further, the attenuation $\tilde{\alpha}$ is proportional to the crack density ε.

We recall that in Angel and Koba (1993) an energy method was used to evaluate the attenuation of antiplane waves in a solid that contains a distribution of parallel cracks. This energy method is valid when the cracks are distant from each other and act as independent scatterers, and when the power scattered by the cracks is small relative to the incident power. When the incident wave is normal to the faces of the cracks, the attenuation in their paper is given by formula (25), which can be written in the form

$$\tilde{\alpha} = \frac{\varepsilon a}{u_0}\,\mathrm{Re}(\bar{B}), \quad \bar{B}a^2 = \int_{-a}^{a} v\bar{b}(v)\,\mathrm{d}v. \tag{76}$$

In (76), the function $\bar{b}$ satisfies eqns (8) and (9) of their paper for $\theta = \pi/2$. Comparing (8) and (9) with (42) and (43), we find that the correspondence between their $\bar{b}$ and our b is given by

$$\bar{b}(v) = iu_0\omega s_T b(v). \tag{77}$$

Then, substituting (77) into (76), we obtain an expression for $\tilde{\alpha}$ that is identical to that of (75). We conclude from this discussion that the attenuation obtained in this paper for small crack densities coincides with the attenuation of Angel and Koba (1993). These authors calculate the velocity $\tilde{c}$ by using (76), the Kramers–Kronig relation (38) of their paper and the condition $\tilde{c}(\infty) = 1$ of their eqn (41). We have verified that their numerical results are identical with those obtained from (72) for small crack densities.

In the limit of high frequency, the results of the next section show that

$$\lim_{\tilde{\omega}\to\infty} B = 0, \quad \lim_{\tilde{\omega}\to\infty} \tilde{\omega}B = -2i. \tag{78}$$

Hence, we infer from (72), (73), and (78) that

$$\lim_{\tilde{\omega}\to\infty} \tilde{c} = 1, \quad \lim_{\tilde{\omega}\to\infty} \tilde{\alpha} = 2\varepsilon, \quad \text{(for all } \varepsilon\text{)}. \tag{79}$$

To find the limits of the transmission coefficient T and of the reflection coefficient R as the frequency approaches infinity, it suffices to substitute (65) into (70) and (71) and to recall (79). Then, one has

$$\lim_{\tilde{\omega}\to\infty} |T| = \exp(-4\varepsilon\tilde{h}), \quad \lim_{\tilde{\omega}\to\infty} |R| = 0. \tag{80}$$

The results (79) can be compared with those of Angel and Koba (1993). One can see that the first result in (79) is identical to that of their equation (41), and the second result in (79) is consistent with the limit $2a\alpha/\varepsilon = 4$ of the curve $\theta_0 = 90°$ in their Fig. 4.

In the limit as the frequency $\tilde{\omega}$ approaches zero, it can be shown that the function $\tilde{S}$ of (64) takes the asymptotic form

$$\tilde{S}(x) = \frac{1}{2} x\tilde{\omega}^2 \log\tilde{\omega} - i\frac{\pi}{4} x\tilde{\omega}^2, \quad \text{as } \tilde{\omega} \to 0. \tag{81}$$

The terms that are neglected in (81) are of $O(\tilde{\omega}^2)$ for the real part and of $O(\tilde{\omega}^4)$ for the imaginary part. Then, using the method of Muskhelishvili (1953), one can find the solution $\tilde{b}$ of (62) and (63) and the number B of (66). To within real terms of $O(\tilde{\omega}^2)$ and imaginary terms of $O(\tilde{\omega}^4 \log\tilde{\omega})$ in the limit as $\tilde{\omega}$ approaches zero, one finds that

$$B = -\frac{\pi}{2} + \frac{\pi}{8}\tilde{\omega}^2 \log\tilde{\omega} - i\left(\frac{\pi\tilde{\omega}}{4}\right)^2, \quad \text{as } \tilde{\omega} \to 0. \tag{82}$$

The values of the velocity $\tilde{c}$ and of the attenuation $\tilde{\alpha}$ in the limit as $\tilde{\omega}$ approaches zero are obtained from (72), (73), and (82). We find the following results

case 1: $\varepsilon < 1/\pi$

$$\tilde{c} = (1-\varepsilon\pi)^{1/2} + O(\tilde{\omega}^2 \log\tilde{\omega}), \quad \tilde{\alpha} = \frac{\varepsilon\pi^2\tilde{\omega}^3}{16(1-\varepsilon\pi)^{3/2}} + O(\tilde{\omega}^5 \log\tilde{\omega}); \tag{83}$$

case 2: $\varepsilon > 1/\pi$

$$\tilde{c} = \frac{16(\varepsilon\pi-1)^{3/2}}{\varepsilon\pi^2\tilde{\omega}^2} + O(\log\tilde{\omega}), \quad \tilde{\alpha} = \frac{\tilde{\omega}}{(\varepsilon\pi-1)^{1/2}} + O(\tilde{\omega}^3 \log\tilde{\omega}). \tag{84}$$

We see from (83) and (84) that the attenuation $\tilde{\alpha}$ always vanishes in the limit as the frequency approaches zero. For $\varepsilon > 1/\pi$, (84) states that the velocity $\tilde{c}$ tends to infinity as the frequency approaches zero, which is not physically acceptable. Thus, we conclude that the results of this paper are valid for small values of the crack density not greater than $1/\pi$. The value $\varepsilon = 1/\pi$ is obtained when each circle of radius a contains on average a crack of width $2a$; or when 4 cracks of width a, or 16 cracks of width $a/2$, are contained on average in each circle of radius a.

We have verified, by using (83), (84), (65), (70) and (71), that in the limit of zero frequency the transmission coefficient tends to 1 and the reflection coefficient to zero. These limits are valid whether ε is less or greater than $1/\pi$.

Next, we examine the amplitudes C and D of (67) and (68). Using (65), one infers that the ratio of the moduli of these quantities is given by

$$|D/C| = M\exp(-2\tilde{h}\tilde{\alpha}), \quad M = |\tilde{K}-\tilde{\omega}|/|\tilde{K}+\tilde{\omega}|, \tag{85}$$

where M does not depend on $\tilde{h}$. We infer from (85) that, for fixed values of $\tilde{\omega}$ and ε, the ratio $|D/C|$ approaches zero as the slab thickness $\tilde{h}$ approaches infinity. This result, together with (47), shows that for large slab thicknesses the forward wave dominates the backward wave at the center of the slab ($y_2 = 0$).

For fixed values of $\tilde{\omega}$ and small values of ε, (85) and (75) imply that

$$M = \frac{\varepsilon}{2}|B| + O(\varepsilon^2), \quad \text{as } \varepsilon \to 0. \tag{86}$$

It follows from (85) and (86) that, for all values of $\tilde{h}$, only the forward wave is significant as the crack density approaches zero. We have verified by using (74), (70), and (71) that in the limit of zero crack density the transmission coefficient tends to 1 and the reflection coefficient to zero.

For fixed values of $\tilde{\omega}$ and small values of $\tilde{h}$, one infers from (69)–(71) and from the boundedness of B (as will be seen in the next section) that T and R are given to within terms of $O(\tilde{h}^2)$ by

$$T = 1-p\tilde{h}, \quad R = p\tilde{h}, \quad p = 2i\tilde{\omega}\varepsilon B/(1+2\varepsilon B), \quad \text{as } \tilde{h} \to 0. \tag{87}$$

Equation (87) shows that the reflection R is proportional to $\tilde{h}$ for small slab thicknesses.

8. NUMERICAL RESULTS

The singular integral eqn (62) and the auxiliary eqn (63) have been approximated by using the method of Erdogan and Gupta (1972), in the case where the unknown function $\tilde{b}$ has square-root singularities at the crack tips. This yields a linear system of equations, which has been solved for 1000 values of the dimensionless frequency $\tilde{\omega}$ equally spaced at intervals of 0.01 in the range [0, 10]. For each frequency, the system consists of 50 complex-valued equations for 50 unknowns.

From (62), (63) and (66), we observe that the quantity B depends only on frequency. Figure 2 shows the real and imaginary parts of $\tilde{\omega}B$ vs the dimensionless frequency $\tilde{\omega}$. At $\tilde{\omega} = 0$, both $\mathrm{Re}(\tilde{\omega}B)$ and $\mathrm{Im}(\tilde{\omega}B)$ vanish. Then, as $\tilde{\omega}$ increases, they decrease until they reach absolute minima, respectively, of -1.8839 at $\tilde{\omega} = 1.08$ and of -2.4541 at $\tilde{\omega} = 1.71$.

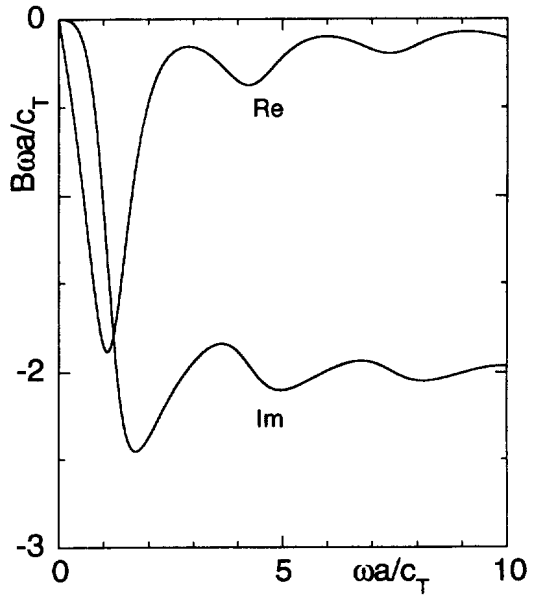

Fig. 2. Real and imaginary parts of $B\omega a/c_T$ vs the frequency.

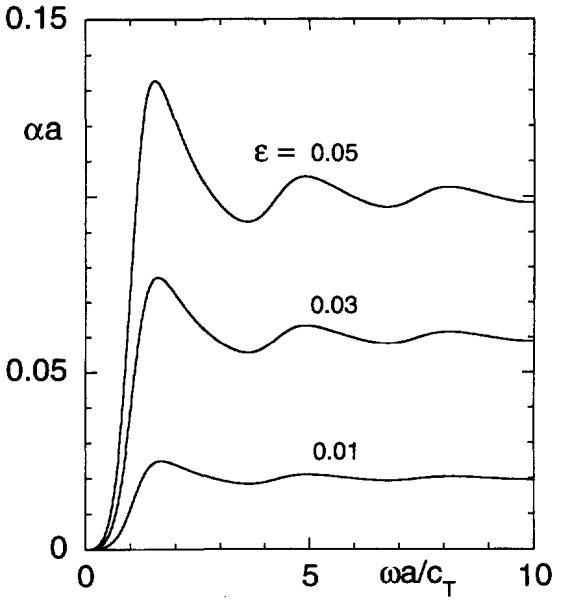

Fig. 3. Attenuation vs the frequency for $\varepsilon = 0.01, 0.03, 0.05$.

Thereafter, the curves have damped oscillations as the frequency increases. The real part approaches the value zero, and the imaginary part the value -2, as stated in (78).

Figure 3 shows the attenuation $\tilde{\alpha}$ vs the dimensionless frequency $\tilde{\omega}$ for crack densities $\varepsilon = 0.01$, 0.03, and 0.05. The curves are obtained by using the formula (72), which has a complicated dependence on ε. The attenuation is maximum at $\tilde{\omega} = 1.68$, 1.62, and 1.55, respectively, for $\varepsilon = 0.01$, 0.03, and 0.05, and the corresponding maxima are 0.024912, 0.077088, and 0.13269. If the approximate formula (75) were used for the attenuation, then the maxima of $\tilde{\alpha}$ would all occur at the frequency $\tilde{\omega} = 1.71$, where $\mathrm{Im}(\tilde{\omega}B)$ is minimum. The curves are very flat near the origin, as expected from the asymptotic limit of $O(\tilde{\omega}^3)$ in (83), and they approach the limits $\tilde{\alpha} = 2\varepsilon$ of (79) as $\tilde{\omega}$ becomes large.

Figure 4 shows the ratio $\tilde{c}$ of the velocity in the cracked region to the velocity in an uncracked solid for crack densities $\varepsilon = 0.01$, 0.03, and 0.05. The curves are obtained by using the formula (72). The value of $\tilde{c}$ at $\tilde{\omega} = 0$ decreases as the crack density increases, in agreement with (83). As the frequency becomes large, the three curves approach the limit

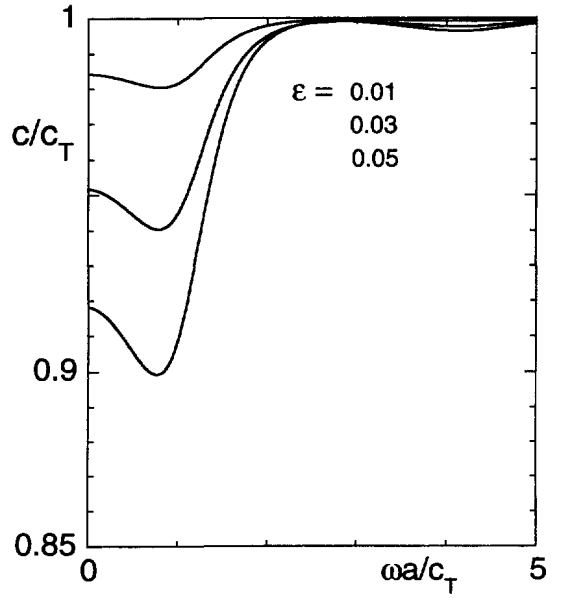

Fig. 4. Velocity vs the frequency for $\varepsilon = 0.01, 0.03, 0.05$.

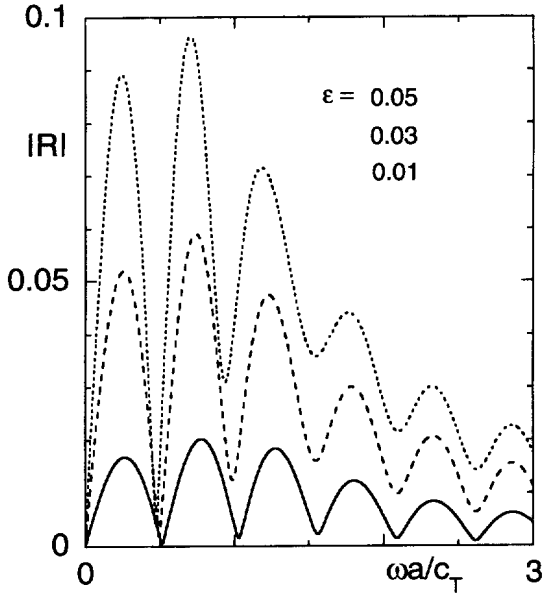

Fig. 5. Modulus of the reflection coefficient vs the frequency for $h/a = 3$ and $\varepsilon = 0.01, 0.03, 0.05$.

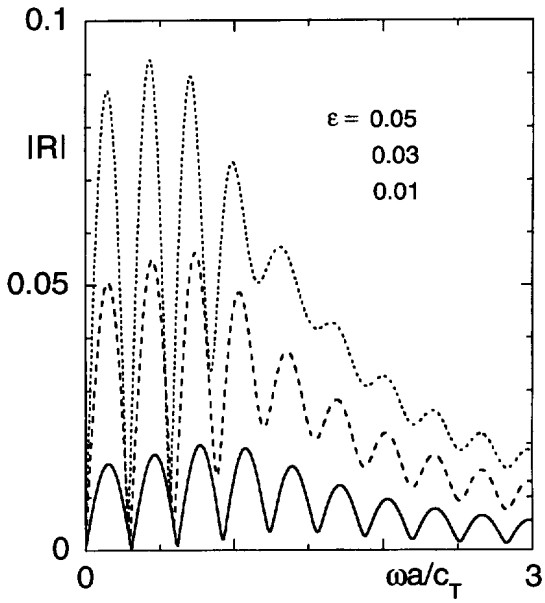

Fig. 6. Modulus of the reflection coefficient vs the frequency for $h/a = 5$ and $\varepsilon = 0.01, 0.03, 0.05$.

$\tilde{c} = 1$ of (79). Each curve has an absolute minimum. These minima are, respectively, 0.98036 at $\tilde{\omega} = 0.81$, 0.94031 at $\tilde{\omega} = 0.79$, and 0.89919 at $\tilde{\omega} = 0.77$, for $\varepsilon = 0.01, 0.03$, and 0.05.

Figures 5 and 6 show the modulus of the reflection coefficient vs the dimensionless frequency for crack densities $\varepsilon = 0.01, 0.03, 0.05$ and thicknesses $\tilde{h} = 3$ and 5, respectively. The curves are obtained by using (71), (65), and (72). The reflection is small (less than 0.1) in both figures. At $\tilde{\omega} = 0$, the value of $|R|$ is zero. Then, as $\tilde{\omega}$ increases, the values of $|R|$ have cyclic variations, which are caused by interference phenomena inside the cracked region. The number of cycles increases noticeably as $\tilde{h}$ increases. The first minimum on each of the six curves occurs at a frequency of approximately $\tilde{\omega} = \pi/(2\tilde{h})$, which corresponds to an incident wave of wavelength $\lambda = 4h$. This wavelength is equal to twice the slab thickness. The following minima occur approximately at wavelengths that are integral multiples of $4h$. The maxima occur approximately between the minima at wavelengths that are equal to $2h$ plus integral multiples of $4h$. Figures 5 and 6 show that the minima and

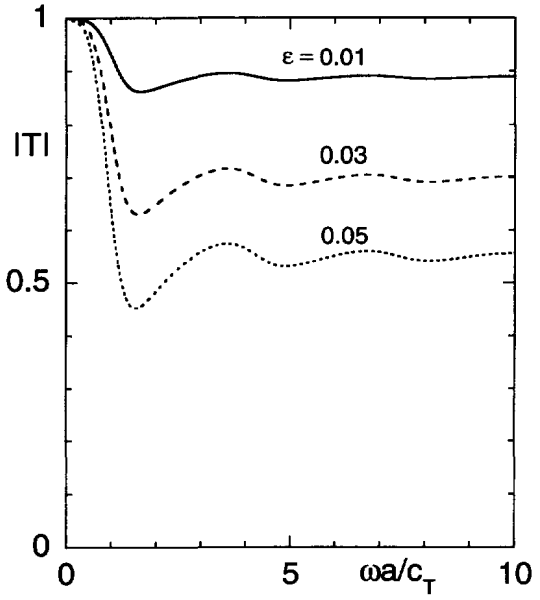

Fig. 7. Modulus of the transmission coefficient vs the frequency for $h/a = 3$ and $\varepsilon = 0.01, 0.03, 0.05$.

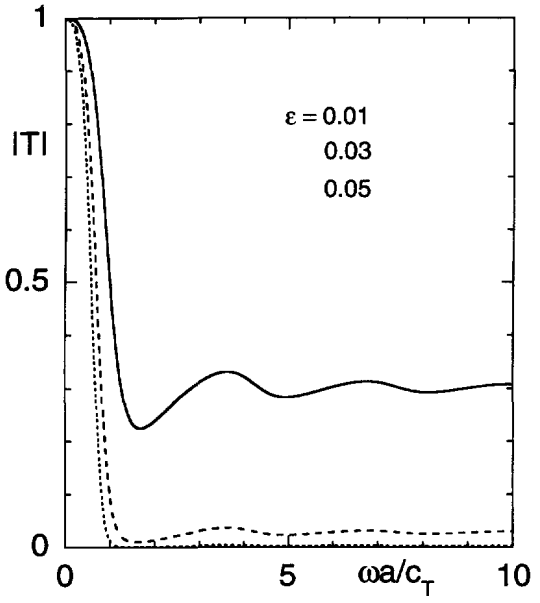

Fig. 8. Modulus of the transmission coefficient vs the frequency for $h/a = 30$ and $\varepsilon = 0.01, 0.03, 0.05$.

maxima are slightly displaced to the left as the crack density increases. As the frequency becomes large, the curves approach the limit $|R| = 0$ of (80).

Figures 7 and 8 show the modulus of the transmission coefficient vs the dimensionless frequency for crack densities $\varepsilon = 0.01, 0.03, 0.05$ and thicknesses $\tilde{h} = 3$ and 30, respectively. The curves are obtained by using (70), (65), and (72). At $\tilde{\omega} = 0$, the value of $|T|$ is 1. Then, as $\tilde{\omega}$ increases, the values of $|T|$ decrease. The decrease is steeper when the crack density ε is larger and when the thickness $\tilde{h}$ is larger. With $\varepsilon = 0.05$ and $\tilde{h} = 30$, the value of $|T|$ drops from 1 to nearly zero as the frequency $\tilde{\omega}$ increases from zero to 1. As the frequency becomes large, the values of $|T|$ approach with damped oscillations the limit $\exp(-4\varepsilon\tilde{h})$ of (80).

We now compare the results of this paper with those of Kikuchi (1981a, b), who also determines a complex-valued wavenumber in a solid containing a distribution of parallel

cracks. His formula, which is given between eqns (14) and (15) in Kikuchi (1981b), can be reproduced using our notation in the form

$$K^2 = k^2/(1+na^2\pi\phi), \tag{88}$$

where the complex-valued quantity ϕ is related to the average crack-opening displacement $\Delta\bar{u}$ by

$$\phi = 2i\Delta\bar{u}/(\pi Ka). \tag{89}$$

The displacement $\Delta\bar{u}$ is that of a crack excited by an antiplane wave of wavenumber K; it can be calculated by using the method discussed by Angel (1988). Then, one finds that ϕ is related to the quantity B of (45) by $\pi\phi = 2B$. We conclude from this discussion that (88) and (48) are identical expressions for the wavenumber K.

The approximate expressions given by Kikuchi in eqn (15) are valid for small values of the crack density ε, and are consistent with (75). The velocity curve in his Fig. 3 is a plot of $(1-\tilde{c})/(\varepsilon\pi)$ vs $\tilde{\omega}$. At zero frequency, the ordinate is 0.5, which is in agreement with the first formula of (83) when a Taylor series expansion of $(1-\varepsilon\pi)^{1/2}$ is taken near $\varepsilon = 0$. For $\tilde{\omega}$ greater than 2, $(1-\tilde{c})$ is less than zero. This is not consistent with the results that we present in Fig. 4, where c is less than c_T for all frequencies. It appears that the numerical inaccuracy of his results is a consequence of evaluating the crack-opening displacement only to within first order terms in frequency.

The attenuation $Q^{-1}/(\varepsilon\pi)$ presented by Kikuchi in Fig. 3 corresponds in our notation to $-2\,\mathrm{Im}(B)/\pi$. We find that the peak value of this last quantity is equal to 1.0162 and occurs at $\tilde{\omega} = 1.41$. In comparison, his peak value and corresponding frequency are 1.2 and 1.3, respectively.

9. CONCLUSIONS

We have investigated the multi-crack problem of elastodynamics where randomly distributed cracks are contained in a slab region of finite thickness. Assuming that an antiplane wave is normally incident on the cracks, which are all identical and parallel to the slab boundaries, we have evaluated the configuration-averaged wave motion inside and outside the slab.

We have used a new method where exact equations and boundary conditions are written for each crack and averaged over all configurations. First, the N-crack problem is considered, where the number N is finite and the cracks are contained in a bounded rectangle. Next, the limit of the averaged N-crack equations is taken as N tends to infinity and the crack number density n is kept constant.

To obtain the limit equations, assumptions have been made concerning the existence of the field quantities in the limit as N tends to infinity and concerning the validity of interchanging the limit operation with differentiations and integrations. Owing to the geometry of the slab, the uniformity of the crack density, and the normal propagation of the incident wave, one infers that the average total displacement in the solid depends only on the coordinate normal to the slab boundaries. For the same reasons, average field quantities associated with a fixed crack must remain invariant when the crack and the observation point are translated by the same amount along the slab length.

In the limit, we find that the average total displacement $\langle u^T\rangle_\infty$ is governed by (36) together with the singular integral eqn (37). When the right-hand side of (37) is known, these are coupled equations for the two scalar unknowns $\langle u^T\rangle_\infty$ and $b(v;\zeta_2)$, where b is related to the average crack-face displacement $\langle u^{sc}\rangle_\infty$ as indicated in eqn (26).

Equation (36) follows directly from (33). This last equation expresses the average total field in terms of a four-fold integral, since J is a double integral with integration variables running along $(-\infty, \infty)$ and $[0, \infty)$, respectively. A representation of $\langle u^T\rangle_\infty$ in terms of a four-fold integral, as in (33), would not be practical, and accurate numerical computations

would be very difficult. We have been able, however, to evaluate J in closed-form; this reduces the four-fold integral to a double integral and yields (36), which proves to be very useful.

Since no assumptions are made regarding crack density, eqns (36) and (37) are valid for all crack densities and take into account all interactions between the cracks. If the average exciting displacement $\langle u^E \rangle_\infty$, which appears in the right-hand side of (37), were known exactly near a fixed crack, then it would be easy to obtain analytically or numerically an exact solution for the average total displacement $\langle u^T \rangle_\infty$.

In the second part of this work, which starts in Section 6, we assume that $\langle u^E \rangle_\infty$ and $\langle u^T \rangle_\infty$ are equal near a fixed crack. This approximation, which is expected to be valid for small concentrations of scatterers, does not have a precisely determined range of validity; however, given (36) and (37), its consequences can be examined thoroughly.

An important consequence is the existence of a complex-valued wavenumber K inside the slab region. The wavenumber K has a simple explicit expression, from which both real and imaginary parts (thus, velocity and attenuation) can be obtained without difficulty. This K was previously determined by Kikuchi (1981a, b), as is discussed in Section 8.

We have further examined the consequences of the assumption that $\langle u^E \rangle_\infty$ is equal to $\langle u^T \rangle_\infty$ near a fixed crack. Our examination reveals that the velocity becomes abruptly unbounded as the crack density reaches a critical value, which corresponds to a distribution with (on average) one crack of width $2a$ in each circle of radius a. Since an unbounded velocity is not physically acceptable, we conclude that our assumption is valid for small (and possibly moderate) values of crack density. In addition, we have obtained analytical limits for vanishingly small crack densities and slab thicknesses that are in agreement with physical intuition; in both cases, the transmission coefficient tends to 1 and the reflection coefficient to zero.

For an acceptable value of the crack density, our analysis is valid in the entire range of frequencies. Numerical results have been obtained at a low cpu-time cost by solving a singular integral equation for each frequency. Our analytical predictions, in particular those for the reflection coefficient, may allow a more accurate interpretation of experimental measurements in ultrasonic nondestructive evaluation and seismic exploration.

Acknowledgements—This material is based in part upon work supported by the Texas Advanced Technology Program under Grant No. 003604-004.

REFERENCES

Angel, Y. C. and Achenbach, J. D. (1991) Attenuation and speed of antiplane waves in a cracked solid using the Kramers–Kronig relations. *Journal of the Acoustical Society of America* **90,** 2757–2762.

Angel, Y. C. (1988) On the reduction of elastodynamic crack problems to singular integral equations. *International Journal of Engineering Science* **26,** 757–764.

Angel, Y. C. and Koba, Y. K. (1993) Propagation of antiplane waves in a multi-cracked solid. In *Anisotropy and Inhomogeneity in Elasticity and Plasticity*, ed. Y. C. Angel, pp. 51–57. AMD-Vol. 158, ASME.

Bose, S. K. (1996) Ultrasonic plane SH wave reflection from a uni-directional fibrous composite slab. *Journal of Sound and Vibration* **193,** 1069–1078.

Erdogan, F. and Gupta, G. D. (1972) On the numerical solution of singular integral equations. *Quarterly Applied Mathematics* **30,** 525–534.

Eriksson, A. S., Boström, A. and Datta, S. K. (1995) Ultrasonic wave propagation through a cracked solid. *Wave Motion* **22,** 297–310.

Foldy, L. L. (1945) The multiple scattering of waves I. General theory of isotropic scattering by randomly distributed scatterers. *Physical Review* **67,** 107–119.

Groenenboom, J. and Snieder, R. (1995) Attenuation, dispersion, and anisotropy by multiple scattering of transmitted waves through distributions of scatterers. *Journal of the Acoustical Society of America* **98,** 3482–3492.

Kerr, F. H. (1992) The scattering of a plane elastic wave by spherical elastic inclusions. *International Journal of Engineering Science* **30,** 169–186.

Kikuchi, M. (1981a) Dispersion and attenuation of elastic waves due to multiple scattering from inclusions. *Physics of the Earth and Planetary Interiors* **25,** 159–162.

Kikuchi, M. (1981b) Dispersion and attenuation of elastic waves due to multiple scattering from cracks. *Physics of the Earth and Planetary Interiors* **27,** 100–105.

Kinra, V. K., Petraitis, M. S. and Datta, S. K. (1980) Ultrasonic wave propagation in a random particulate composite. *International Journal of Solids and Structures* **16,** 301–312.

Kinra, V. K. and Anand, A. (1982) Wave propagation in a random particulate composite at long and short wavelengths. *International Journal of Solids and Structures* **18,** 367–380.

Koba, Y. K. (1996) Average antiplane motion in an elastic solid containing a layer of randomly distributed cracks. Ph.D. dissertation, Rice University, Houston, Texas, U.S.A.
Kuga, Y., Rice, D. and West, R. D. (1996) Propagation constant and the velocity of the coherent wave in a dense strongly scattering medium. *IEEE Transactions on Antennas and Propagation* **44,** 326–332.
Lax, M. (1951) Multiple scattering of waves. *Reviews of Modern Physics* **23,** 287–310.
Lax, M. (1952) Multiple scattering of waves II. The effective field in dense systems. *Physical Review* **85,** 621–629
McCarthy, M. F. and Carroll, M. M. (1984) Multiple scattering of SH waves by randomly distributed dissimilar scatters. In *Wave Phenomena: Modern Theory and Applications*, C. Rogers, and T. B. Moodie, pp. 433–451. Elsevier (North-Holland), The Netherlands.
Muskhelishvili, N. I. (1953) *Singular Integral Equations*. P. Noordhoff, Groningen, The Netherlands.
Peacock, S., McCann, C., Sothcott, J. and Astin, T. R. (1994a) Seismic velocities in fractured rocks: an experimental verification of Hudsons' theory. *Geophysical Prospecting* **42,** 27–80.
Peacock, S., McCann, C., Sothcott, J. and Astin, T. R. (1994b) Experimental measurements of seismic attenuation in microfractured sedimentary rock. *Geophysics* **59,** 1342–1351.
Sayers, C. M. and Smith, R. L. (1983) Ultrasonic velocity and attenuation in an epoxy matrix containing lead inclusions. *Journal of Physics D: Applied Physics* **16,** 1189–1194.
Sneddon, I. N. (1972) *The Use of Integral Transforms*. McGraw-Hill, New York.
Twersky, V. (1962) On scattering of waves by random distributions. I. Free-space scatterer formalism. *Journal of Mathematical Physics* **3,** 700–715.
Varadan, V. K., Ma, Y. and Varadan, V. V. (1989) Scattering and attenuation of elastic waves in random media. *Pure and Applied Geophysics* **131,** 577–603.
Waterman, P. C. and Truell, R. (1961) Multiple scattering of waves. *Journal of Mathematical Physics* **2,** 512–537.
Zhang, Ch. and Achenbach, J. D. (1991) Effective wave velocity and attenuation in a material with distributed penny-shaped cracks. *International Journal of Solids and Structures* **27,** 751–767.
Zhang, Ch. and Gross, D. (1993a) Wave attenuation and dispersion in randomly cracked solids—I. Slit cracks. *International Journal of Engineering Science* **31,** 841–858.
Zhang, Ch. and Gross, D. (1993b) Wave attenuation and dispersion in randomly cracked solids—II. Penny-shaped cracks. *International Journal of Engineering Science* **31,** 859–872.

APPENDIX

The integral J, which is defined in (34), is evaluated in closed form. One has

$$\int_{-X}^{X} P(v, y_2, \zeta)\, \mathrm{d}\zeta_1 = -\int_{-X}^{X} \left\{ \int_0^{\infty} \frac{1}{\xi} \sin\left[\xi(\zeta_1 + v)\right] \exp\left(-\beta|y_2 - \zeta_2|\right) \mathrm{d}\xi \right\} \mathrm{d}\zeta_1. \tag{A.1}$$

Evaluating the ζ_1 integral in (A.1), one finds that

$$\int_{-X}^{X} P(v, y_2, \zeta)\, \mathrm{d}\zeta_1 = -2 \int_0^{\infty} \frac{1}{\xi^2} \sin(\xi v) \sin(\xi X) \exp\left(-\beta|y_2 - \zeta_2|\right) \mathrm{d}\xi. \tag{A.2}$$

The limit of the above integral as X tends to infinity can be obtained by using the localization lemma (Sneddon, 1972, pp. 32–33) and the definition of the function β in (30). Since $\beta = -ik$ at $\xi = 0$, one infers from (A.1), (A.2) and (34) that

$$J(v, y_2, \zeta_2) = -\pi v\, \mathrm{sgn}(y_2 - \zeta_2) \exp\left(ik|y_2 - \zeta_2|\right). \tag{A.3}$$

This proves the result (35).